# Estimating preseason irrigation losses by characterizing evaporation of effective precipitation under bare soil conditions using large weighing lysimeters

Gary Marek [a,*], Prasanna Gowda [b], Thomas Marek [c], Brent Auvermann [d], Steven Evett [a], Paul Colaizzi [a], David Brauer [a]

[a] USDA-ARS, Conservation and Production Research Laboratory, P.O. Drawer 10, Bushland, TX 79012, United States
[b] USDA-ARS, Forage and Livestock Production Research Unit, 7207 West Cheyenne Street, El Reno, OK 73036, United States
[c] Texas A&M AgriLife Research, 6500 Amarillo Blvd. West, Amarillo, TX 79106, United States
[d] Texas A&M AgriLife Research & Extension, 6500 Amarillo Blvd. West, Amarillo, TX 79106, United States

## ARTICLE INFO

## ABSTRACT

Irrigation from the Ogallala aquifer is used to supplement insufficient precipitation for agricultural crop production in the semi-arid Texas High Plains. Decreased pumping capacity has compelled many producers to "pre-water" fields to field capacity prior to planting to hedge against pumping limitations later in the season. However, the direct measurement of evaporative losses from preseason irrigation of bare soil is not commonly studied. The quantification of evaporative losses from effective precipitation, or the net amount of water that infiltrates into the soil following a precipitation event, can be used as a surrogate for estimating losses from preseason irrigation. We identified 35 precipitation events that occurred over lysimeter fields under fallow conditions in 2002, 2005, and 2009. Events were categorized into four bins of precipitation magnitude ranging from 3 mm to 35 mm. Subsequent evaporation was measured for a period of up to seven days following rainfall events using large weighing lysimeters at the USDA-ARS Conservation and Production Research Laboratory in Bushland, TX. An exponential decay function was used to characterize bare soil evaporation using maximum cumulative measured evaporation ($E_{Cmax}$), soil water transfer constant ($k$), and cumulative grass reference evapotranspiration ($ET_{Cos}$). The wide range of $E_{Cmax}$ values and $k$ values demonstrated the sensitivity of evaporative losses to both antecedent soil water content and evaporative demand. We also present measured average daily evaporation values for a range of evaporative demand regimes for each precipitation bin. From data analyzed in this study, nearly all of the water from precipitation events of 10 mm and less were lost to evaporation within the following day under moderate to high grass reference evapotranspiration ($ET_{os}$) conditions. Nearly all water from precipitation events between 20 and 30 mm was lost to evaporation between three to four days following the event under similar evaporative demand. The considerable potential evaporative losses from preseason irrigation call into the question the prudence of the preseason irrigation, particularly for regions with limited groundwater resources.

© 2016 Published by Elsevier B.V.

## 1. Introduction

Irrigation from the Ogallala aquifer is used to supplement insufficient precipitation for agricultural crop production in the semi-arid Texas High Plains. Decades of pumping combined with low recharge have decreased the saturated thickness of the aquifer resulting in decreased well yields. Decreased pumping capacity compels affected agricultural producers to maximize crop yield while minimizing irrigation inputs (Pittman et al., 2007). This may be achieved by increasing water use efficiency (WUE) through the use of more efficient irrigation systems, and by implementing more effective irrigation management and alternate cropping strategies. Many producers, however, are unable or unwilling to invest in new irrigation infrastructure given the downward trend in well capacities in some areas. They are more likely to focus on and continue to adopt improved irrigation scheduling and alternate cropping systems. Research on management strategies that shift a

* Corresponding author at: P.O. Drawer 10, 2300 Experiment Station Rd., Bushland, TX 79012, United States.
E-mail address: gary.marek@ars.usda.gov (G. Marek).
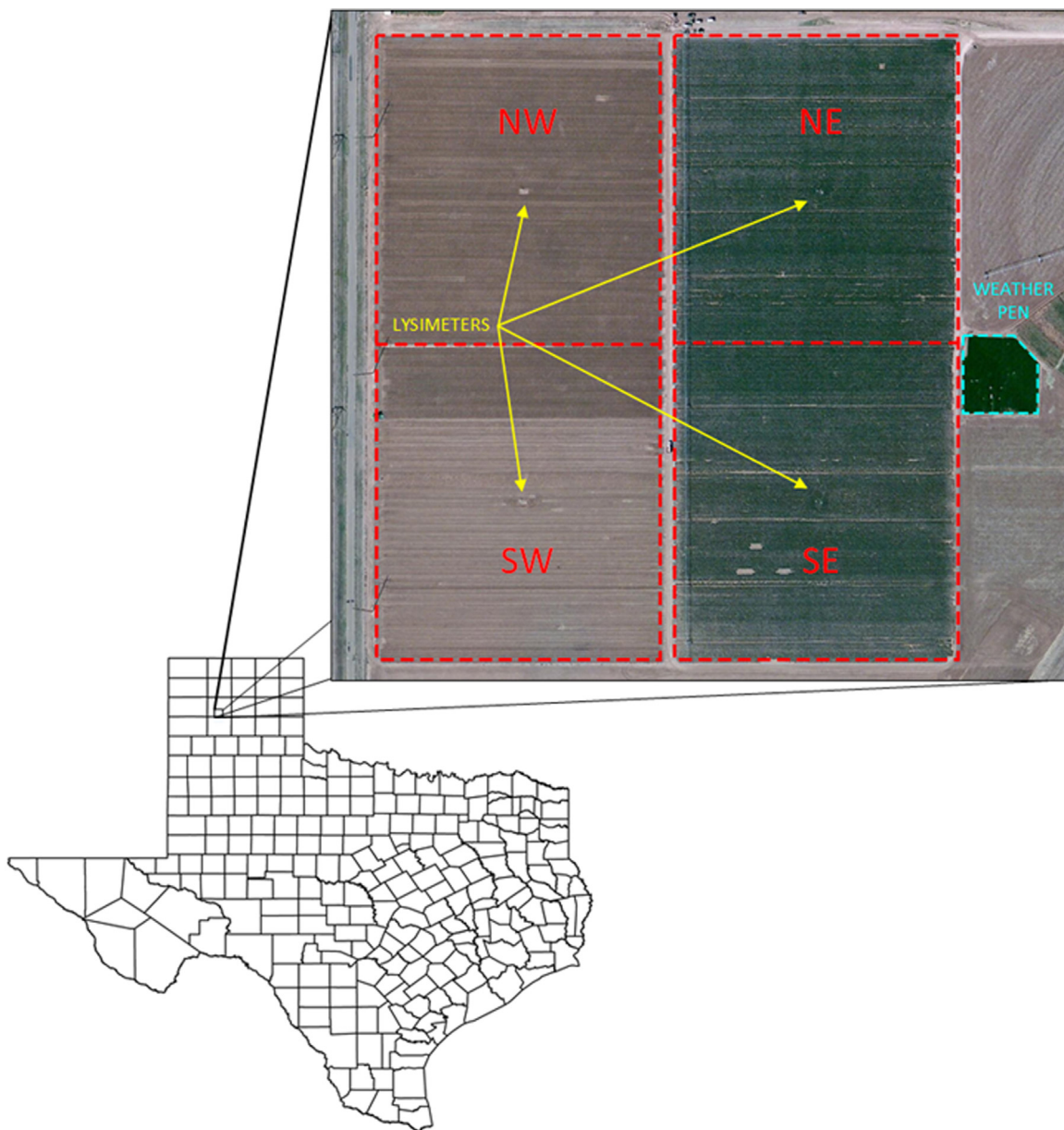
**Fig. 1.** Location and orientation of four weighing lysimeters fields and the weather pen at USDA-ARS CPRL in Bushland, TX.

**Table 1**
Selected soil parameters and values for Pullman clay loam soils at Bushland, TX.

| Depth (mm) | 0–180 | 180–860 | 860–1800 | 1800–2300 |
|---|---|---|---|---|
| Bulk density (g cm$^{-3}$) | 1.23 | 1.46 | 1.48 | 1.41 |
| Available water capacity (mm H$_2$O per mm soil) | 0.15 | 0.15 | 0.15 | 0.14 |
| Saturated hydraulic conductivity (mm h$^{-1}$) | 5.72 | 2.16 | 2.16 | 5.16 |
| Clay content | 30.3 | 37.4 | 38.4 | 37.4 |
| Silt content | 49.3 | 45.0 | 41.2 | 42.1 |
| Sand content (% soil mass) | 20.4 | 17.6 | 20.4 | 20.5 |

**Table 2**
Precipitation event statistics measured from the NW and SW lysimeters in 2002, 2005, and 2009.

| Precipitation ($P$) magnitude (mm) | Number of measurements | Minimum precip. (mm) | Maximum precip. (mm) | Mean precip. (mm) | Median precip. (mm) | Std. deviation (mm) |
|---|---|---|---|---|---|---|
| $3 < P < 10$ | 19 | 3.7 | 9.8 | 8.2 | 9.1 | 1.9 |
| $10 \leq P < 20$ | 28 | 10.1 | 17.9 | 13.5 | 13.0 | 2.7 |
| $20 \leq P < 30$ | 11 | 23.1 | 29.3 | 26.2 | 26.0 | 2.1 |
| $P \geq 30$ | 8 | 31.5 | 37.3 | 33.6 | 33.7 | 2.0 |

**Table 3**
Coefficient of determination ($r^2$) and soil water transfer constant ($k$) values for drying events by precipitation bin.

| | 3 < P < 10 | | | 10 ≤ P < 20 | | | 20 ≤ P < 30 | | | P ≥ 30 < 40 | |
|---|---|---|---|---|---|---|---|---|---|---|---|
| | $k$ | $r^2$ | | $k$ | $r^2$ | | $k$ | $r^2$ | | $k$ | $r^2$ |
| 1 | −0.6751 | 0.9862 | 1 | −0.0677 | 0.9947 | 1 | −0.2102 | 0.9975 | 1 | −0.0677 | 0.9942 |
| 2 | −0.2460 | 0.9812 | 2 | −0.2659 | 0.9907 | 2 | −0.2179 | 0.9968 | 2 | −0.0676 | 0.9850 |
| 3 | −0.1001 | 0.9977 | 3 | −0.1654 | 0.9858 | 3 | −0.0966 | 0.9888 | 3 | −0.0545 | 0.9891 |
| 4 | −0.1233 | 0.9821 | 4 | −0.2721 | 0.9920 | 4 | −0.1014 | 0.9937 | 4 | −0.0601 | 0.9924 |
| 5 | −0.1371 | 0.9764 | 5 | −0.1797 | 0.9886 | 5 | −0.0874 | 0.9907 | 5 | −0.047 | 0.9829 |
| 6 | −0.9150 | 0.9869 | 6 | −0.0970 | 0.9937 | 6 | −0.0827 | 0.9918 | 6 | −0.0455 | 0.9852 |
| 7 | −0.0949 | 0.9828 | 7 | −0.1524 | 0.9983 | 7 | −0.0641 | 0.9955 | 7 | −0.0569 | 0.9942 |
| 8 | −0.0728 | 0.9815 | 8 | −0.1063 | 0.9879 | 8 | −0.0495 | 0.9876 | 8 | −0.0674 | 0.9941 |
| 9 | −0.0542 | 0.9974 | 9 | −0.1089 | 0.9881 | 9 | −0.0552 | 0.9876 | | | |
| 10 | −0.0553 | 0.9961 | 10 | −0.0780 | 0.9899 | 10 | −0.0421 | 0.9690 | | | |
| 11 | −0.0429 | 0.9769 | 11 | −0.0814 | 0.9824 | 11 | −0.0587 | 0.9730 | | | |
| 12 | −0.0381 | 0.9917 | 12 | −0.0817 | 0.9885 | | | | | | |
| 13 | −0.0396 | 0.9903 | 13 | −0.0866 | 0.9891 | | | | | | |
| 14 | −0.0403 | 0.9807 | 14 | −0.0727 | 0.9462 | | | | | | |
| 15 | −0.0658 | 0.9800 | 15 | −0.0576 | 0.8682 | | | | | | |
| 16 | −0.0455 | 0.9569 | 16 | −0.0870 | 0.9813 | | | | | | |
| 17 | −0.0455 | 0.9574 | 17 | −0.0887 | 0.9916 | | | | | | |
| 18 | −0.0876 | 0.9467 | 18 | −0.0787 | 0.9886 | | | | | | |
| 19 | −0.2273 | 0.9829 | 19 | −0.0823 | 0.9861 | | | | | | |
| | | | 20 | −0.0435 | 0.9880 | | | | | | |
| | | | 21 | −0.0432 | 0.9919 | | | | | | |
| | | | 22 | −0.0414 | 0.9862 | | | | | | |
| | | | 23 | −0.0403 | 0.9872 | | | | | | |
| | | | 24 | −0.1206 | 0.9939 | | | | | | |
| | | | 25 | −0.1265 | 0.9463 | | | | | | |
| | | | 26 | −0.0814 | 0.9488 | | | | | | |
| | | | 27 | −0.0978 | 0.8623 | | | | | | |
| | | | 28 | −0.2881 | 0.9930 | | | | | | |
| Min | −0.9150 | | | −0.2721 | | | −0.2179 | | | −0.0677 | |
| Max | −0.0381 | | | −0.0403 | | | −0.0421 | | | −0.0428 | |
| Range | 0.8769 | | | 0.2318 | | | 0.1758 | | | 0.0249 | |
| Avg | −0.1600 | | | −0.1039 | | | −0.0969 | | | −0.0550 | |

**Table 4**
Precipitation ($P$) magnitude and cumulative maximum evaporation ($E_{Cmax}$) values by precipitation bin.

| | 3 < P < 10 | | | 10 ≤ P < 20 | | | 20 ≤ P < 30 | | | P ≥ 30 | |
|---|---|---|---|---|---|---|---|---|---|---|---|
| | $P$ | $E_{Cmax}$ | | $P$ | $E_{Cmax}$ | | $P$ | $E_{Cmax}$ | | $P$ | $E_{Cmax}$ |
| 1 | 9.1651 | 17.9 | 1 | 17.001 | 11.3 | 1 | 27.850 | 18.5 | 1 | 34.331 | 15.6 |
| 2 | 6.8394 | 15.5 | 2 | 16.732 | 11.4 | 2 | 29.300 | 21.3 | 2 | 33.312 | 21.7 |
| 3 | 7.8051 | 14.0 | 3 | 12.094 | 17.7 | 3 | 28.138 | 15 | 3 | 31.488 | 20.3 |
| 4 | 8.4882 | 12.7 | 4 | 12.775 | 16.9 | 4 | 23.112 | 17.5 | 4 | 34.180 | 21.3 |
| 5 | 9.8411 | 10.8 | 5 | 11.353 | 4.1 | 5 | 25.636 | 19.6 | 5 | 37.336 | 18.2 |
| 6 | 9.1890 | 10.5 | 6 | 12.149 | 4.5 | 6 | 23.824 | 11.8 | 6 | 31.507 | 22.3 |
| 7 | 9.6567 | 2.0 | 7 | 13.289 | 15.3 | 7 | 23.077 | 12.2 | 7 | 31.597 | 18.7 |
| 8 | 6.6104 | 4.9 | 8 | 13.723 | 15.8 | 8 | 26.045 | 10.9 | 8 | 34.766 | 19.3 |
| 9 | 6.3717 | 5.2 | 9 | 15.430 | 12.5 | 9 | 26.045 | 13.2 | | | |
| 10 | 8.6642 | 7.9 | 10 | 10.327 | 11.4 | 10 | 27.699 | 12.8 | | | |
| 11 | 8.9853 | 7.3 | 11 | 10.520 | 11.1 | 11 | 27.640 | 11.6 | | | |
| 12 | 9.4699 | 10.1 | 12 | 10.208 | 5.4 | | | | | | |
| 13 | 3.7218 | 11.4 | 13 | 10.192 | 9.5 | | | | | | |
| 14 | 3.8858 | 11.5 | 14 | 10.116 | 9.5 | | | | | | |
| 15 | 9.5803 | 18.1 | 15 | 10.660 | 6.8 | | | | | | |
| 16 | 9.5803 | 18.2 | 16 | 10.577 | 9.7 | | | | | | |
| 17 | 9.0986 | 9.5 | 17 | 10.674 | 10.3 | | | | | | |
| 18 | 9.3179 | 9.4 | 18 | 14.715 | 10.8 | | | | | | |
| 19 | 9.4164 | 10.4 | 19 | 14.863 | 11.6 | | | | | | |
| | | | 20 | 12.558 | 11.9 | | | | | | |
| | | | 21 | 16.811 | 11.0 | | | | | | |
| | | | 22 | 17.313 | 10.2 | | | | | | |
| | | | 23 | 16.967 | 10.1 | | | | | | |
| | | | 24 | 16.852 | 10.1 | | | | | | |
| | | | 25 | 17.873 | 19.4 | | | | | | |
| | | | 26 | 17.439 | 10.6 | | | | | | |
| | | | 27 | 12.498 | 12.9 | | | | | | |
| | | | 28 | 13.448 | 14.2 | | | | | | |
| Min | | 2.0 | | | 4.1 | | | 10.9 | | | 15.6 |
| Max | | 18.2 | | | 19.4 | | | 21.3 | | | 22.3 |
| Range | | 16.2 | | | 15.3 | | | 10.4 | | | 6.7 |
| Avg | | 10.9 | | | 11.3 | | | 14.9 | | | 19.7 |
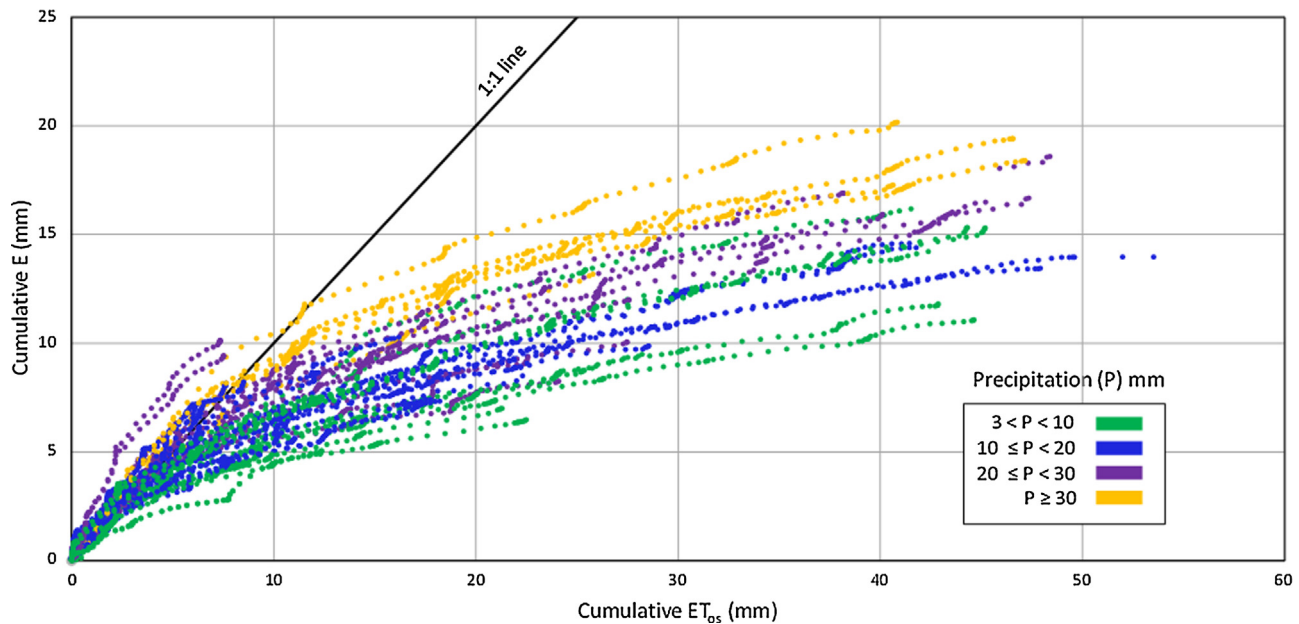
**Fig. 2.** Cumulative grass reference evapotranspiration (ET$_{Cos}$) and cumulative measured evaporation ($E_C$) for all precipitation events.

proportion of irrigated lands to dryland or deficit irrigation regimes is becoming more prevalent as groundwater resources decline (Baumhardt et al., 2009; Hernandez et al., 2013). These advanced management strategies may be complemented by incorporating systematic El Niño Southern Oscillation (ENSO) patterns used to predict weather patterns including precipitation in North America (Baumhardt et al., 2015). Allocating limited irrigation resources to a larger percentage of acreages during years when increased precipitation is predicted could maximize production. Conversely, irrigation water could be concentrated by reducing irrigated acres during projected periods of drought or less than average rainfall, reducing the risk of crop failure of larger acreages. Variable rate center pivot irrigation systems now available can make reallocation to different sized areas much easier than in the past (O'Shaughnessy et al., 2013, 2015). Shifting to less water-intensive crops such as cotton has also been viewed as a way to maintain profitability with decreased irrigation capacity (Moorhead et al., 2013). However, the recent influx of dairies to the Texas Panhandle has placed a premium on water-intensive forage crops such as corn (*Zea mays*) and sorghum (*Sorghum bicolor*) silages and even alfalfa (*Medicago sativa*). Producers growing these crops often irrigate prior to planting to fill the soil profile to "hedge" against their decreased pumping capacity later in the season. This practice, however, is not always a "certain bet" or sound irrigation practice as the quantification of water beneficial to crop production later is not always known.

Few studies have directly measured the evaporative losses associated with the preseason irrigation of bare soils. However, losses to evaporation from bare soils can be significant, particularly in the early growing season when canopy cover is incomplete and losses are dependent upon the duration of time between application and use (Evett et al., 2015; Tolk et al., 2015). Effective precipitation is largely ambiguous in the literature and largely dependent upon agronomic and climatic contexts. For example, a light rainfall event (∼5 mm) following a crop planting in an upper soil zone containing marginal water content can be important to ensuring seed germination and subsequent root development into deeper soil moisture. Small precipitation events such as these are particularly significant or "effective" in semi-arid regions when near surface soil water quickly evaporates between precipitation events. However, that same event occurring later in the growing season under high evap-

otranspiration (ET) conditions is almost negligible in terms of total seasonal water use for a water-intensive crop even though it may fall during a full crop canopy context. Irrespective of qualification, the appreciable water from precipitation is affected by the magnitude of the event, intensity, surface runoff, soil hydraulic properties, evapotranspiration, and antecedent soil moisture. Increased evaporation can also occur following tillage operations due to both increased vapor flow and increased absorption of solar radiation due to reduced albedo (Schwartz et al., 2010). Soil structure effects associated with tillage can also affect drying rates from bare soil. Knowledge of soil water dynamics and water partitioning at and near the soil surface is required for accurate modeling of evaporation. The distribution of soil water near the soil surface changes quickly and can be challenging to measure accurately, requiring significant instrumentation and data processing effort. For the purposes of this work under bare soil conditions, effective precipitation can be defined as the net amount of water that infiltrates into the soil following a precipitation event. We propose that measurements of evaporative losses of effective precipitation can be used as a surrogate for estimating effective irrigation from the prewatering of bare soil. Characterization of effective precipitation under bare soil conditions could be useful for estimating evaporative losses associated with preseason irrigation practices in the Texas High Plains and other regions with similar soils and climate. We evaluated empirical bare soil evaporation data following rainfall events of varying magnitude collected from two large weighing lysimeters located at the USDA-ARS Conservation and Production Research Laboratory in Bushland, TX from 2002, 2005, and 2009. We present and evaluate an alternative approach for estimating bare soil evaporation using minimal soil parameters, precipitation events, and calculated reference evapotranspiration. We also present a summary of pooled evaporation data sorted by precipitation and subsequent ET demand.
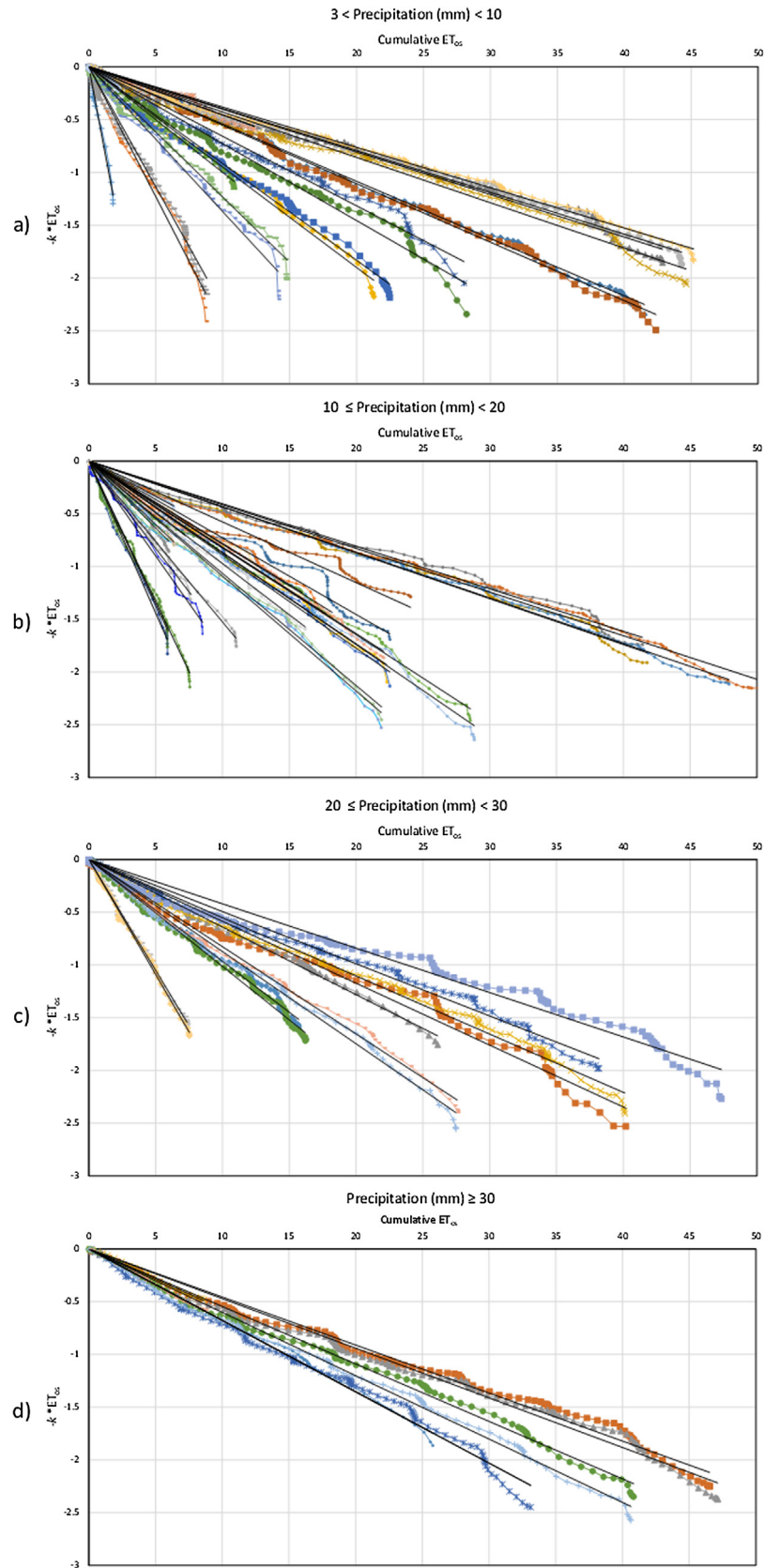
## 2. Materials and methods

### 2.1. Study area

The study area consists of a square ∼20 ha research field located at the USDA-ARS Conservation and Production Research Labora-
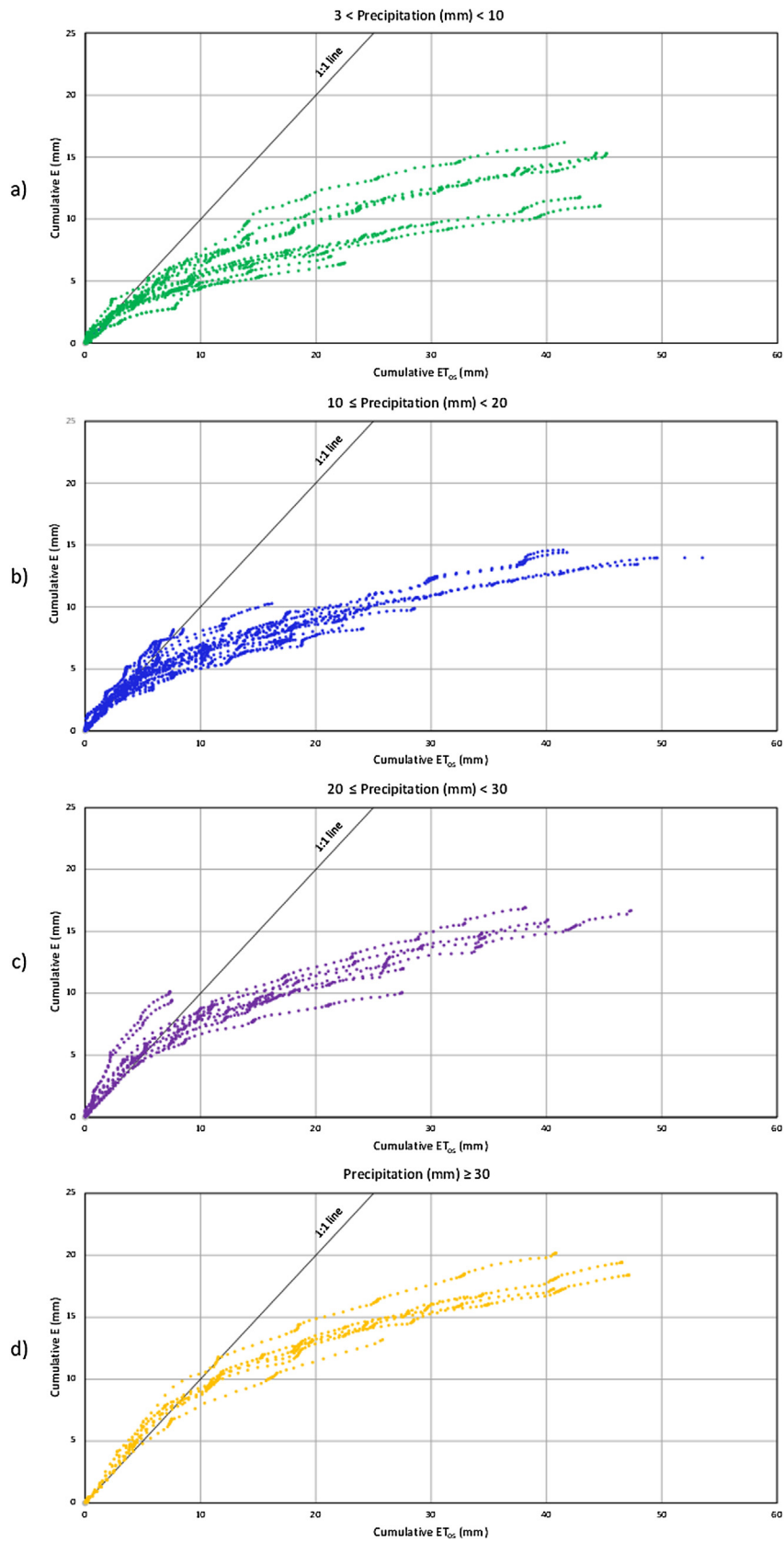
**Fig. 3.** Cumulative measured evaporation ($E_C$) and cumulative grass reference evapotranspiration ($ET_{Cos}$) for precipitation (P) bins of (a) 3 mm < P < 10 mm, (b) 10 mm ≤ P < 20 mm, (c) 20 mm ≤ P < 30 mm, and (d) P ≥ 30 mm.

**Fig. 4.** Log transformed plots of $-kET_{os}$ versus $ETC_{os}$ for precipitation (P) bins of (a) 3 mm < P < 10 mm, (b) 10 mm ≤ P < 20 mm, (c) 20 mm ≤ P < 30 mm, and (d) P ≥ 30 mm.

tory (CPRL) at Bushland, TX (35.19° N, 102.10° W, 1170 m elev. above mean sea level). The field is subdivided into four square 4.7 ha fields, each having a weighing lysimeter located in its center and

each designated according to its position relative to the cardinal points as either NE, SE, NW or SW (Fig. 1). Adjacent to the east side of the lysimeter fields is a 1760 m² irrigated, mowed reference
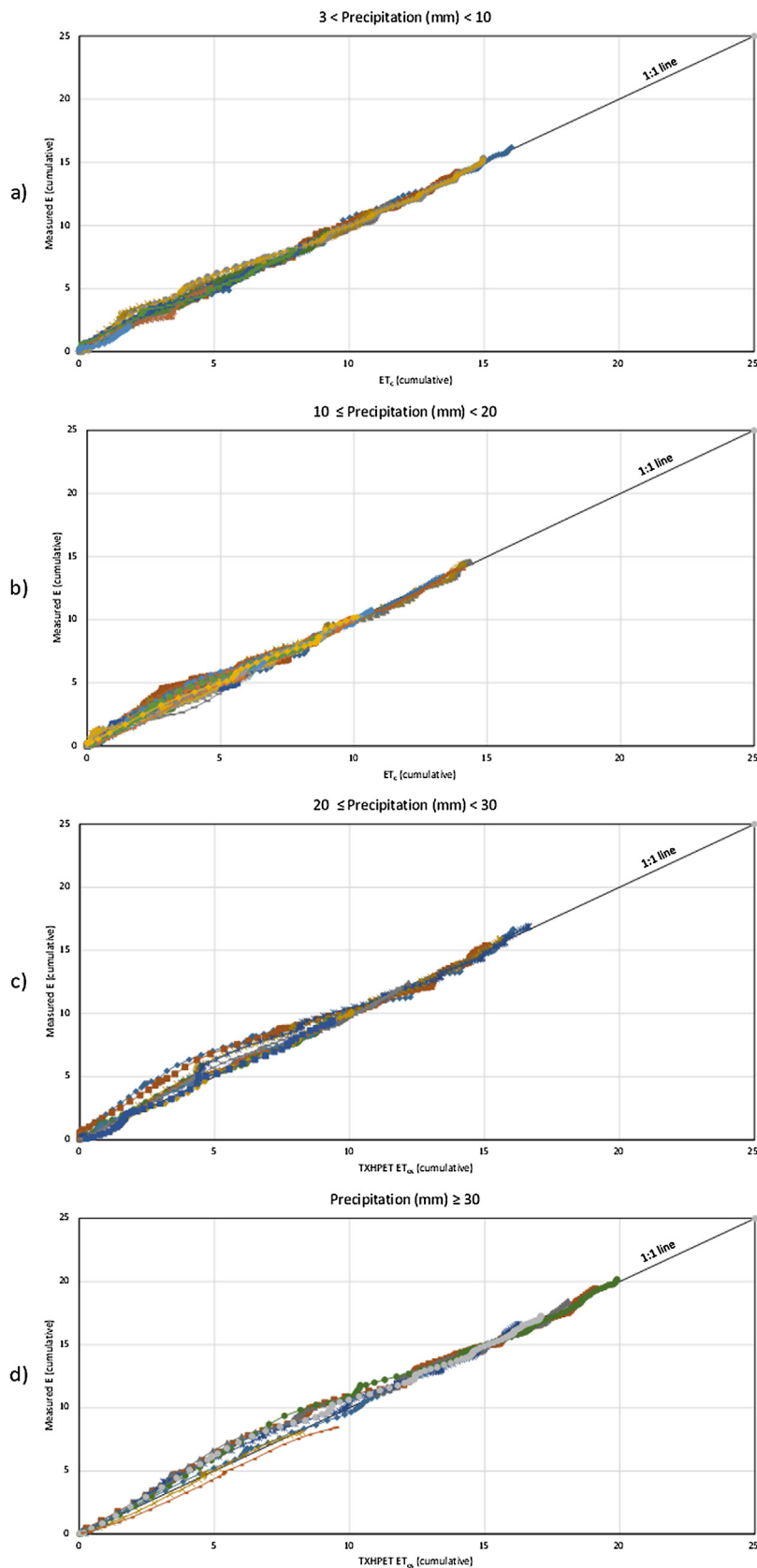
**Fig. 5.** Comparison of calculated ($\hat{E}_C$) and measured ($E_C$) cumulative evaporation.

ET grass plot with a research weather station with instrumentation described by Evett et al. (2012a) and maintained in accordance with ASCE-EWRI specifications (Allen et al., 2005). The study area consists of deep, well drained Pullman silty clay loam (fine, mixed, superactive, thermic Torrertic Paleustoll) (NRCS, 2015; Unger and Pringle, 1981). Measured soil properties for a profile depth of 2.3 m
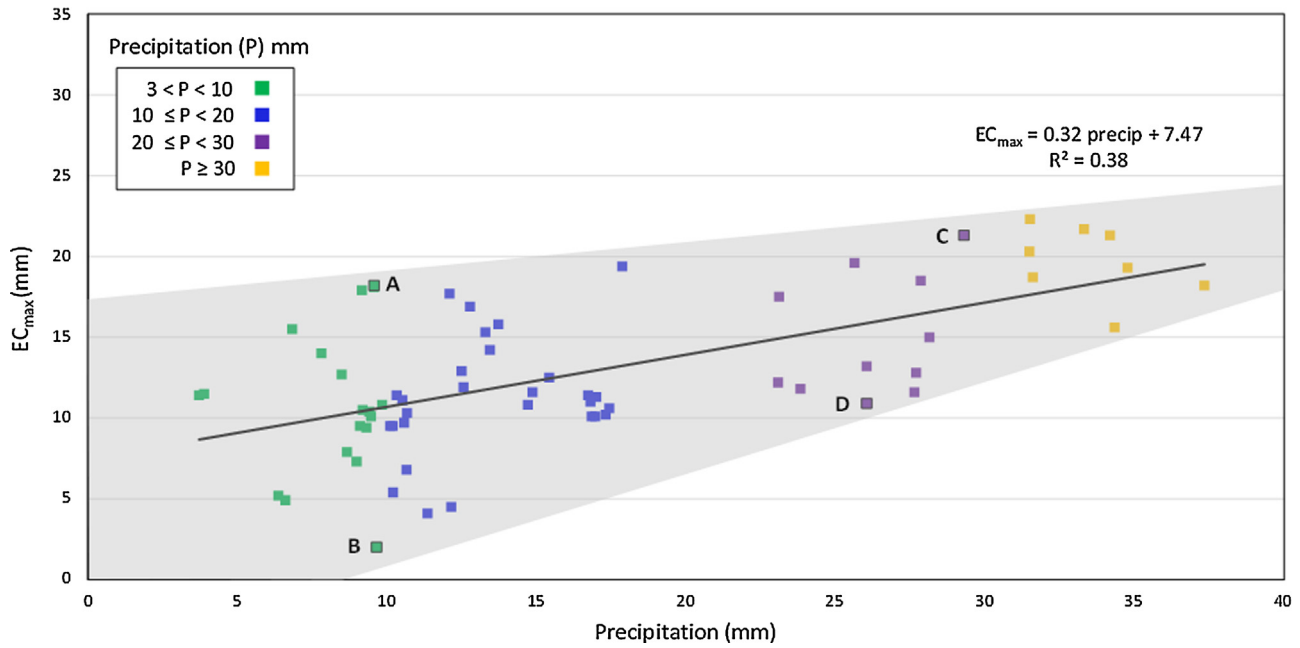
**Fig. 6.** Values of maximum cumulative evaporation ($E_{Cmax}$) versus precipitation by precipitation bin.
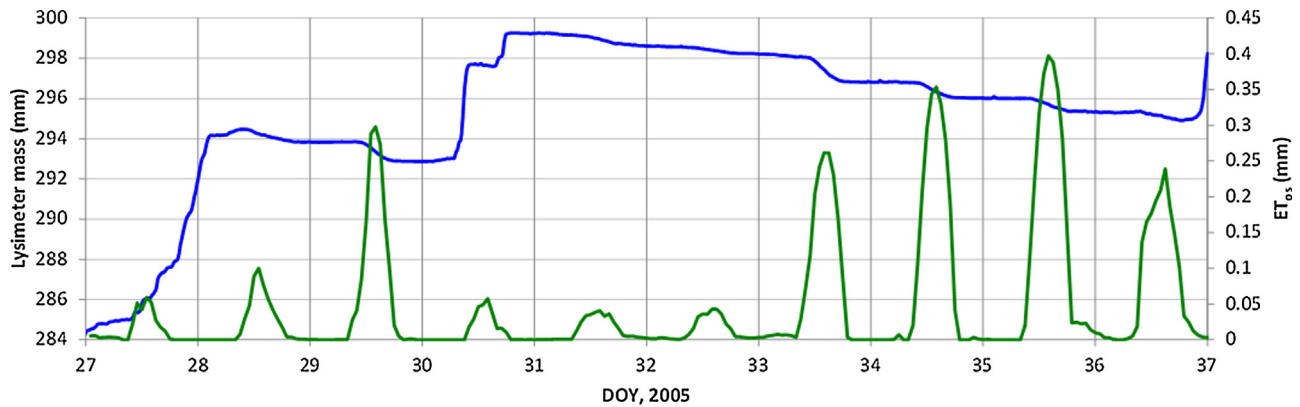


**Fig. 7.** Lysimeter mass response to precipitation events on DOY 27-28 and DOY 30 on the NW lysimeter in 2005. Corresponding hourly grass reference evapotranspiration ($ET_{os}$) is plotted on the secondary axis.
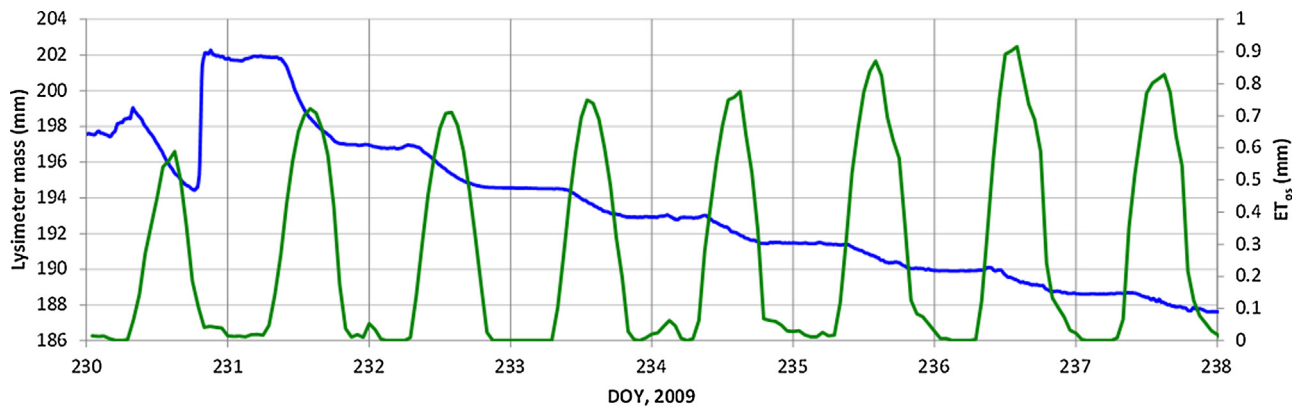


**Fig. 8.** Drying associated with prolonged high hourly grass reference evapotranspiration ($ET_{os}$) following a precipitation event on DOY 230 on the NW lysimeter in 2009.

for the Pullman clay loam soils at Bushland are provided in Table 1. Lysimeter fields were sized to have fetches from lysimeters to field edges in the predominant S-SW upwind direction that would minimize the effects of advection on lysimeter ET and microclimate instrumentation values. Fields slope to the east at ∼0.15% (Dusek et al., 1987) and are typically furrow diked to minimize runoff. The local climate is classified as semiarid characterized by large diurnal temperature variations and day-to-day variability, often caused
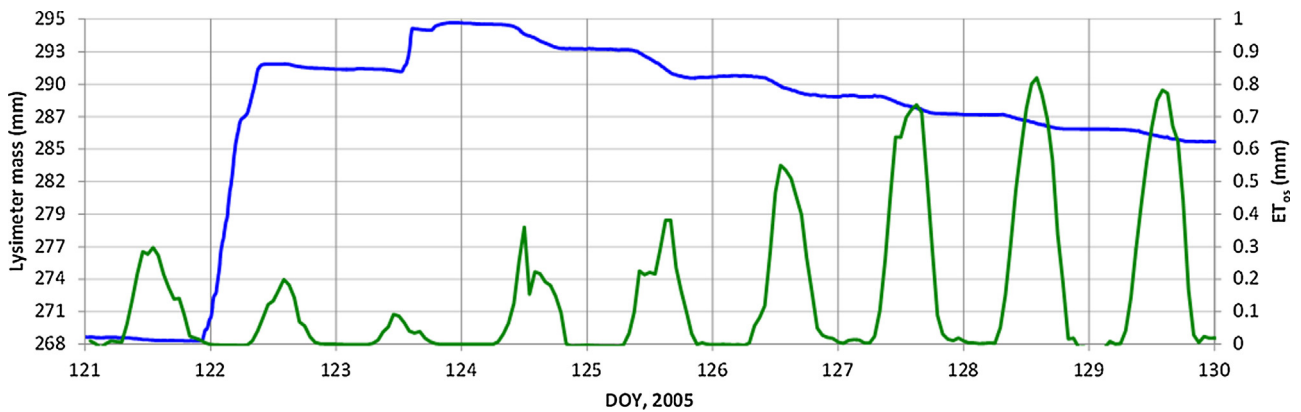
**Fig. 9.** NW lysimeter storage and hourly grass reference evapotranspiration ($ET_{os}$) following a prolonged precipitation event on DOY 121-124 in 2005.
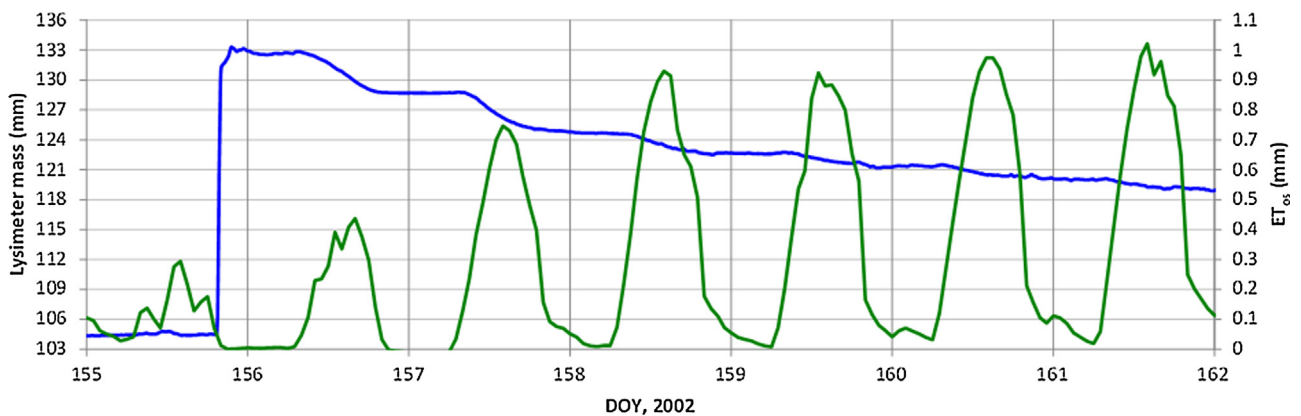


**Fig. 10.** Minimal drying of the SW lysimeter following a high intensity, short duration precipitation event on DOY 155 in 2002, suggesting a lack of antecedent soil water.
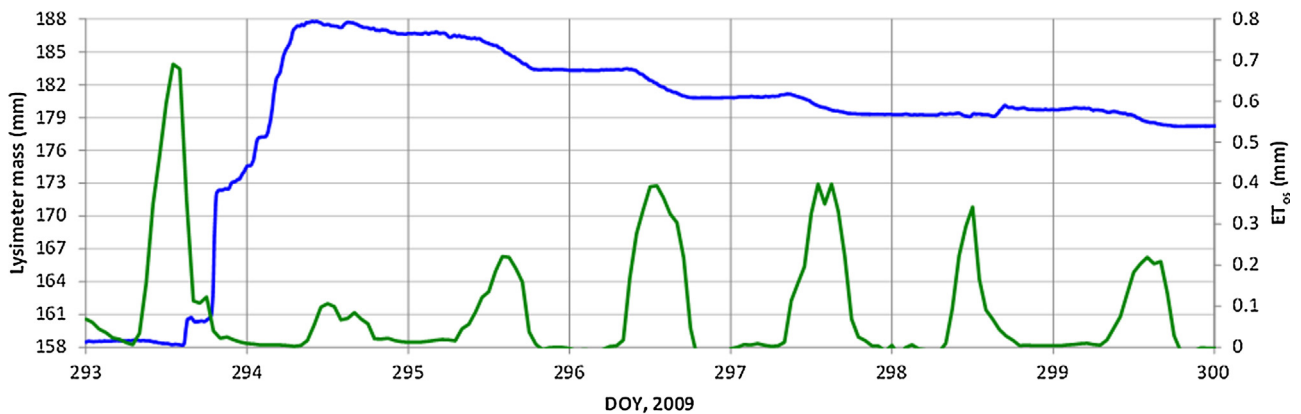


**Fig. 11.** SW lysimeter mass reflecting evaporation greater than that of cumulative grass reference evapotranspiration ($ET_{Cos}$) under relatively low hourly grass reference evapotranspiration ($ET_{os}$) values following a precipitation event on DOY 293 in 2009.

by cold fronts moving southward from the northern Great Plains. The east fields typically received irrigation treatments while the west fields were often managed as dryland. However, in some years the fields were left to fallow to allow for cropping rotations or other research needs. Data collected from the NW and SW lysimeters from 2002, 2005, and 2009 fallow years were used in this study. Management of the lysimeters and fields during fallow years included shredding of stalks from the previous year's crop and subsequent tillage as needed for weed control. The 2002 and 2009 fallow years were preceded by dryland cotton crops and the 2005 year was preceded by a dryland grain sorghum crop.

### 2.2. Lysimeter design & management

Each of the four lysimeters contains an undisturbed monolith of Pullman clay loam, weighing approximately 45 Mg including the container mass. Soil monoliths were necessary to preserve the dense Bt horizon located approximately in the 0.3–0.9 m depth range below the surface and the underlying calcic horizon of substantially different soil hydraulic properties. Lysimeter surface dimensions are approximately $3 \times 3$ m $(9\,m^2)$ and have a soil monolith depth of 2.3 m over a fine sand drainage base. The lysimeter
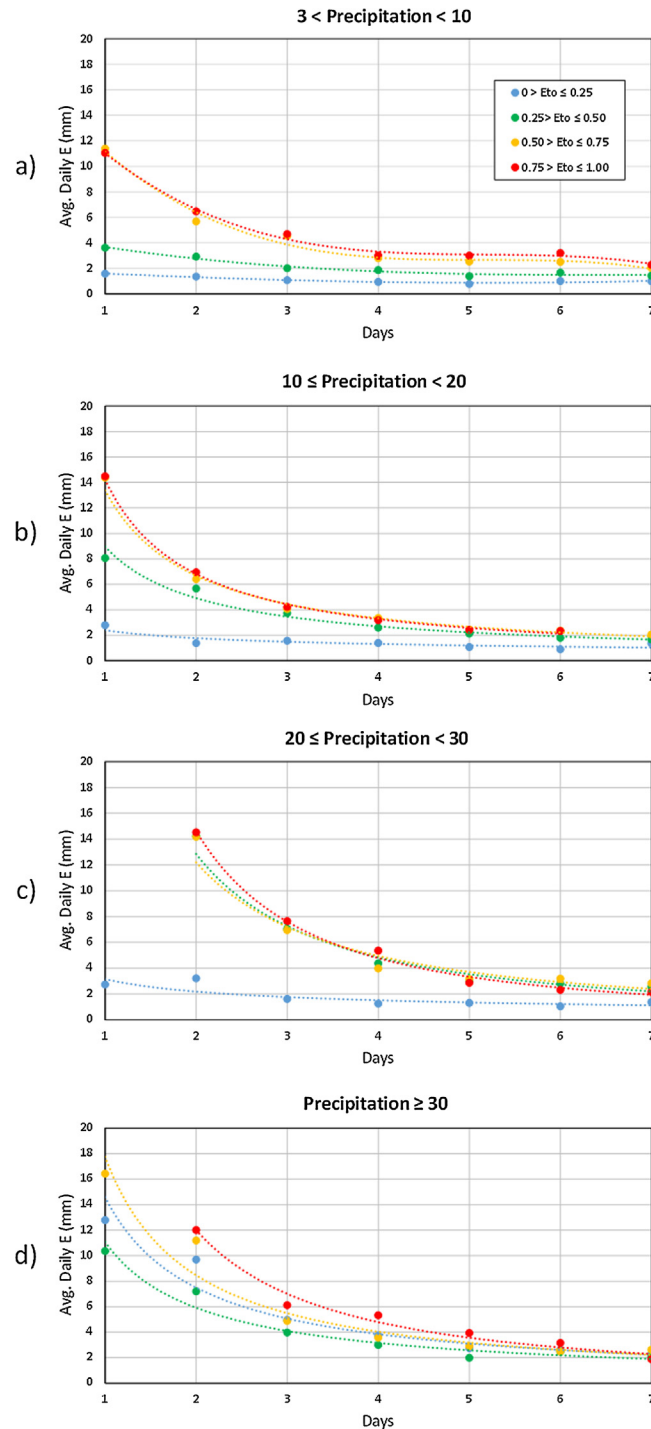
**Fig. 12.** Daily evaporation totals by hourly grass reference evapotranspiration ($ET_{os}$) regime following precipitation event bins.

scales are Cardinal Manufacturing FS-7[1] agronomy scales with 100:1 mechanical advantage. Each lysimeter is equipped with drainage effluent tanks suspended from the lysimeter by load cells for separate measurement of drainage mass without changing total lysimeter mass. Initial design, construction, and installation details were provided by Marek et al. (1988) and Schneider et al. (1988). Voltage outputs from Interface SM-50[1] (Interface Inc., Scottsdale,

AZ) load cells with 22 kg full-range capacity were measured and recorded by CR-7X[1] (Campbell Scientific, Logan, UT) data loggers at 0.5-Hz (2 s) frequency. The lysimeter datalogger mass resolution is better than 0.001 mm when converted to equivalent depth of water. Lysimeter accuracy is, however, determined by the RMSE of calibration, which has ranged from 0.05 mm to 0.01 mm (Howell et al., 1995; Evett et al., 2012b). Experienced support scientists and technicians are responsible for maintaining lysimeter representativeness of surrounding fields. Careful attention is given to agronomic operations including planting, harvesting, tillage, fertilization, irrigation, plant sampling, soil water measurements (neutron scattering), and pesticide application such that there

---

[1] Disclaimer: mention of trade names or commercial products in this manuscript is solely for the purpose of providing specific information and does not imply recommendation or endorsement by the U.S. Department of Agriculture.

should be no distinguishable difference between the crop grown on the lysimeter and that grown in the surrounding field. This also insures that the lysimeter surfaces are representative of the surrounding fields during times of fallow. Changes in lysimeter mass are used to quantify the addition (precipitation) and loss (evaporation) of water from the lysimeter soil monolith. Lyismeter load cell voltage outputs are converted to mass using calibration equations, and five-minute means are used to develop a base dataset for subsequent processing (Howell et al., 1995). Lysimeter mass in kg is converted to a mass-equivalent relative lysimeter storage value (mm of water) by dividing it by the relevant surface area of the lysimeter ($\sim$9 m$^2$) and the density of water (taken as 1000 kg m$^{-3}$). In the case of bare soil or fallow studies with no plant stand, the relevant surface area is that determined by the inside dimensions of the lysimeter monolith container. Evett et al. (2012b) reported that the Bushland lysimeter inside surface area was 8.95 m$^2$. Equivalent mass values allow for changes in lysimeter mass to be expressed in terms of water flux, defined as mm of water lost or gained per unit time.

### 2.3. Precipitation identification and characterization

Precipitation in the context of this paper is defined as liquid phase rainfall and excludes snowfall and ice events. The challenges of measuring evaporation following snowfall and ice events, particularly those resulting in drifts that are subjected to freeze thaw cycles, are detailed by Marek et al. (2014). Precipitation events were manually identified and quantified from lysimeter mass datasets using post-processing analysis methods described by Marek et al. (2014). Both the occurrence and magnitude of rainfall events were corroborated by tipping bucket rain gauge data collected at the lysimeter and/or weather pen. Hourly evaporation was calculated by subtracting hourly-centered, five-minute values following each event. The evaluation period following each precipitation event was determined by the transition from increasing lysimeter mass to decreasing mass up to a maximum of seven days following the event. Not all events had an associated full seven days of data following an event due to the occurrence of subsequent precipitation events, lysimeter maintenance operations, or data acquisition failure. Precipitation magnitude was calculated by the summation of flagged increases in lysimeter storage values as described in Marek et al. (2014). In some instances, a series of precipitation events over the course of a day, each followed by short drying times, was treated as a singular precipitation event. In these cases precipitation magnitude was calculated by summing positive changes in lysimeter storage and subtracting the evaporated water from the episodic drying periods. In most cases each precipitation event was recorded by both the NW and SW lysimeters, which provided two independent measures of each precipitation event. However, in some instances events were recorded by only one lysimeter due to maintenance or data acquisition problems with the second lysimeter. Sixty-six measurements of 35 precipitation events were selected as suitable for use in this study and analyzed. Precipitation events occurred in all seasons of the year. Seven events occurred between January–March while ten occurred between April–June. Twelve and eight events occurred between July–September and October–December respectively. It should be understood that precipitation event statistics are used to assess the discussed methodologies and that there are effectively two measurements of each event so data should not be interpreted as a distribution of precipitation occurrence and magnitude.

Hourly lysimetric evaporation data following precipitation events were compared to synchronous hourly grass reference evapotranspiration (ET$_{os}$) data from a Texas High Plains ET Network (Marek et al., 2005) research weather station maintained in accordance with ASCE-EWRI (2005) specifications. The ET$_{os}$ values were computed using the Penman–Monteith reference evapotranspiration equation (ASCE, 2005). This approach allows for the comparison of measured evaporation to ET$_{os}$, a term that incorporates the evaporative demand potential of temperature, wind speed, and solar radiation, the primary drivers of evaporation. In this way, the effect of time is not considered as time alone following a precipitation event has no reliable correlation to evaporative demand.

## 3. Results and discussion

### 3.1. Data analysis

Thirty-five rainfall events that occurred during the fallow years of 2002, 2005, and 2009 were identified and quantified. Precipitation events were categorized by magnitude ($P$) into bins of 3 mm< $P$ < 10 mm, 10 mm ≤ $P$ < 20 mm, 20 mm ≤ $P$ < 30 mm, and $P$ ≥ 30 mm (Table 2). Precipitation events less than 3 mm were not considered. Cumulative measured evaporation ($E_C$) and cumulative grass reference evapotranspiration (ET$_{Cos}$) for each event were plotted (Fig. 2). Data series containing fewer points than others represent events that did not contain a full seven days of data due to aforementioned reasons. The diurnal effects of solar radiation and air temperature are evident in the diurnal "stair step" changes in slope of the cumulative plots, while the gradual decrease of soil water available for evaporation is reflected in the gradual decrease in maximum daily slope. The $E_C$ and ET$_{Cos}$ for each event by precipitation bin were plotted for clarity (Fig. 3). Measured evaporation commonly exceeded ET$_{os}$ during stage one (S1) evaporation directly following precipitation events. This is typical of stage one drying of bare soil under energy limited conditions. Tolk et al. (2015) reported S1 evaporation from bare soils exceeded ET$_{os}$ on the day of irrigations by an average of 21% for a clay loam, silt loam, sandy loam, and fine sand at Bushland. Similar rates for all four textures indicated that soil texture had no significant effect on E:ET$_o$ ratio during S1. Allen et al. (2005) previously proposed that S1 E could exceed ET$_o$ by 15% when substituting a reference ET$_o$ for potential evaporation.

Cumulative E:ET$_{os}$ plots illustrate a similar general shape for all four precipitation bins (Fig. 3). The totals of $E_C$ for precipitation events <20 mm were similar, generally between 10–15 mm. (Fig. 3a and b). The $E_C$ values for precipitation between 20 and 30 mm trended slightly larger than those of the two smaller bins (Fig. 3c) while $E_C$ for precipitation events ≥30 mm were the largest. Two data series representing one precipitation event in the 20 ≤ $P$ < 30 mm bin displayed $E_C$ values that exceeded ET$_{Cos}$ values by more than any other event (Fig. 3c, see two leftmost curves).

### 3.2. Estimating evaporation

The $E_C$:ET$_{Cos}$ plots approximated the general form of an increasing exponential decay function where $E_C$ approaches an upper bound or maximum cumulative evaporation ($E_{Cmax}$). The $E_{Cmax}$ value for each event is determined by the amount of water available for evaporation at and near the soil surface, which is essentially the sum of rainfall magnitude and antecedent soil moisture content, although Tolk et al. (2015) point out that texture-dependent soil hydraulic conductivity does mediate the amount of soil water available for evaporation since water can move deeply more quickly in sandier soils. We proposed that $E_{Cmax}$ could be approximated from ET$_{Cos}$ using the following equation.

$$\hat{E}_C = E_{C\,max}(1 - e^{-k\mathrm{ET}_{Cos}}) \tag{1}$$

where $\hat{E}_C$ is the estimated cumulative evaporation in mm, $E_{Cmax}$ is maximum cumulative evaporation in mm, $k$ is a soil water transfer

constant, and $ET_{Cos}$ is the cumulative grass reference ET in mm. The soil water transfer constant is an empirical value that represents the rate of transfer of soil available water to the atmosphere in response to available energy. As $E_{Cmax}$ and $k$ are sensitive to soil water content and soil water partitioning they must be determined for each event. Values of $E_{Cmax}$ and $k$ were estimated for each event by log transforming each data series using the following equation.

$$-kET_{Cos} = \ln\left(\frac{E_{C\,max} - E_C}{E_{C\,max}}\right) \qquad (2)$$

where $E_C$ is measured cumulative evaporation. Plotting the transformed data resulted in near-linear data series of negative slope (Fig. 4). Linear regression trend lines were applied to each series. The $E_{Cmax}$ values were determined using an iterative, manual approach to maximize $r^2$ values of the linear regressions for each series. The slope of the regression line associated with each optimized $E_{Cmax}$ was set to $k$ (Table 3). The $k$ values displayed a wide degree of variation overall but decreased with increasing precipitation (Fig. 4). Similarly, the range of $E_{Cmax}$ decreased with increasing precipitation while the mean value increased (Table 4). Values of $\hat{E}_C$ were plotted versus $E_C$ in order to assess the efficacy of the exponential decay approach. As expected, the resulting graphs indicated good agreement between the values for all precipitation bins (Fig. 5).

We then plotted $E_{Cmax}$ against precipitation magnitude for all events to determine any relationship between the two (Fig. 6). A linear regression resulted in poor correlation ($r^2 = 0.38$) as considerable scatter exists throughout the data series. However, closer inspection reveals an envelope in which the variation in $E_{Cmax}$ decreases as precipitation magnitude increases. We supposed that as the magnitude of precipitation increases, the impact of antecedent soil moisture and its spatial variability decreases, resulting in less variation in $E_{Cmax}$. We therefore proposed that events having an $E_{Cmax}$ greater than that of the precipitation event suggest the presence of both available antecedent soil water and cumulative $ET_{os}$ in excess of the precipitation event. Points having an $E_{Cmax}$ less than that of the precipitation magnitude indicate $ET_{Cos}$ being less than the precipitation amount.

We investigated four points in Fig. 6 associated with precipitation events having larger and smaller $E_{Cmax}$ values for events approximately 25% and 75% of the range of precipitation values. Lysimeter mass and $ET_{os}$ following precipitation were used to surmise antecedent moisture conditions by evaluating mass response to $ET_{os}$ conditions. It is important to note that changes in lyimeter mass reflect changes in total water storage and provide no direct indication of soil water partitioning throughout the lysimeter soil profile, particularly near the surface in the evaporating zone.

Point A (Fig. 6) indicates an $E_{Cmax}$ of 2.0 mm for a 9.66 mm rainfall event that ended in the morning of day of year (DOY) 28 of 2005 on the NW lysimeter. A plot of lysimeter mass following the event revealed low daily ET for DOY 28 with corresponding low $E$ for DOY 28 (Fig. 7). Increased $ET_{os}$ for DOY 29 resulted in increased $E$ as well. The evaluation period for this event was truncated due to a subsequent rainfall event that occurred on DOY 30. An $E_{Cmax}$ of 4.9 mm for this 6.61 mm event was larger than that of the previous smaller precipitation event. The second precipitation event was followed by two days of relatively small $ET_{os}$ followed by increased daily $ET_{os}$ for DOY 33-36. Acknowledging the unknown antecedent soil moisture prior to DOY 28, it is reasonable to assume that adequate soil water was present prior to the second precipitation event due to the short period of time between the two events and resulting in the overall increase in lysimeter mass associated with low $ET_{os}$ conditions leading up to the second event. The data following the precipitation on DOY 30 provide evidence that $E_{Cmax}$ can be significantly less than that of the precipitation event if subsequent $ET_{os}$ is small even if adequate soil water is available. This supports the hypothesis that events having an $E_{Cmax}$ smaller than the precipitation magnitude are the result of limited energy rather than limited soil water.

Point B (Fig. 6) represents a larger $E_{Cmax}$ of 18.2 mm associated with a 9.58 mm rainfall event that occurred on the NW lysimeter on DOY 230 in 2009. This high intensity, short duration rainfall event was corroborated by data from the rain gage located in the adjacent weather pen. A plot of lysimeter mass indicates the event was followed by seven days of uninterrupted drying having days of approximately equal, relatively large $ET_{os}$ (Fig. 8). The most significant decrease in lysimeter mass occurred between noon and the evening hours of the following day leading to cumulative $E$ equaling the magnitude of the precipitation event by the end of the second day. Drying occurred over the next 5 days to a total of approximately 6.8 mm. This suggests that antecedent soil water content contributed toward the portion of $E_{Cmax}$ that was greater than the precipitation amount. This indicates points having $E_{Cmax}$ larger than precipitation magnitude can represent scenarios with adequate antecedent soil water to satisfy relatively large $ET_{os}$ following the complete evaporation of water from the precipitation event.

Point C (Fig. 6) represents a 10.9 mm $E_{Cmax}$ associated with a 26.0 mm precipitation event that occurred on the NW lysimeter on DOY 121-123 in 2005. A plot of lysimeter mass following the event revealed increasing $ET_{os}$ for days 122–128 (Fig. 9). Daily evaporation totals decreased over time but remained significant throughout the evaluation period. Total evaporated water during the evaluation period totaled approximately 38% of the precipitation. This was likely related to the small $ET_{os}$ following the precipitation event allowing for percolation of water deeper into the profile. Once the water had moved lower in the profile and the surface dried out, the water was not as easily evaporated under stage two drying when $ET_{os}$ increased days later. This provides evidence that relatively small $E_{Cmax}$ values associated with larger precipitation events can imply that some of the precipitation water was lost to percolation.

Point D (Fig. 6) represents a 21.3 mm $E_{Cmax}$ associated with a 29.3 mm precipitation event that occurred on DOY 155 on the SW lysimeter in 2002. A plot of lysimeter mass following the event revealed increasing $ET_{os}$ for days 156–158 at which relatively large $ET_{os}$ was sustained throughout the remainder of the evaluation period (Fig. 10). However, daily total evaporation leveled off after DOY 158 and $E_{Cmax}$ totaled only 42% of the precipitation event. Similar to point C, percolation to lower soil depths may account for the seemingly low $E$ associated with $ET_{os}$ demand following the event.

The data series demonstrating the greatest $E$:$ET_{os}$ ratio of 1.38 (7.35 mm of $E$ versus 10.13 mm of $ET_{os}$) was associated with a 27.7 mm precipitation event that occurred on DOY 293-294 on the SW lysimeter (Fig. 11). This event is represented graphically by the leftmost data series occurring the farthest above the $E$:$ET_{os}$ 1:1 line in Fig. 3c. The short duration, high intensity rainfall represented by the steep increase in lysimeter mass in the evening of DOY 293 was verified by tipping bucket rainfall gauges and a similar increase in mass for NW lysimeter storage mass. Daily minimum temperatures did not reach freezing. However, the combination of soil and atmospheric conditions surrounding the event appears to be conducive to bare soil evaporation far larger than what $ET_{os}$ would suggest.

### 3.3. Evaporation of effective precipitation

Measured lysimeter evaporation data within the four precipitation bins were filtered by hourly average $ET_{os}$ bins. Hourly average $ET_{os}$ bins were defined as $0 < ET_{os} < 0.25$ mm, $0.25\ \text{mm} \leq ET_{os} < 0.5$ mm, $0.5\ \text{mm} \leq ET_{os} < 0.75$ mm, and $0.75\ \text{mm} \leq ET_{os} < 1.0$ mm. The average hourly measured evaporation associated with each $ET_{os}$ bin was multiplied by 24 to

generate a daily evaporation loss value for each day following the precipitation event. Due to the filtering, the resulting trend lines do not represent continuous data from individual series but rather a composite plot of data points that satisfy the filter criteria (Fig. 12). Plots that are missing data points are due to the lack of data that meet the filter criteria. For instance, in Fig. 12d, there were no instances of average hourly $ET_{os}$ for the 0.5 mm $\leq ET_{os} <$ 0.75 mm, and 0.75 mm $\leq ET_{os} <$ 1.0 mm regimes for the day following precip events $\geq$30 mm so there were no corresponding lysimeter evaporation data. The resulting plots may provide useful guidelines for estimating losses from effective precipitation values that can be correlated to losses from pre-watering irrigation under bare soil conditions. For example, the 24 h evaporative demand of approximately 11 mm under moderate to high $ET_{os}$ (0.5–1.00 mm hr$^{-1}$ avg.) would evaporate all water from precipitation events between 3 and 10 mm (Fig. 12a). However, approximately 4 and 2 mm would be lost in the first 24 h under small (0.25–0.5 mm hr$^{-1}$ avg.) and very small (0.0–0.25 mm hr$^{-1}$ avg.) $ET_{os}$ regimes respectively. In agreement with Tolk et al. (2015), evaporation following precipitation events greater than 30 mm under high evaporative demand may approach 20 mm within 24 h, followed by 12 and 6 mm for the next two days. Evaporation for the same event under very small $ET_{os}$ conditions will be approximately 10 mm in the first day followed by 7 and 4 mm for the following two days respectively.

## 4. Conclusions

Evaporation of water from bare soil is dependent upon a complex interaction of intrinsic soil properties, atmospheric conditions, and precipitation magnitude. Knowledge of antecedent moisture in the upper surface layer of the soil would likely have increased utility of the precipitation to $E_{Cmax}$ relationship. However the availability of such data for analysis is extremely limited. The development of accurate, wireless soil water content sensors may prove useful for in situ evaporation measurements. This work demonstrates the sensitivity of antecedent soil water content and associated soil water partitioning to bare soil evaporation processes. The summary of an evaluation of pooled data from all precipitation events provides estimates for evaporation loss by precipitation $ET_{Cos}$ magnitudes. From data analyzed in this study, nearly all of precipitation events of 10 mm and less are lost to evaporation within the following day under moderate to high $ET_{os}$ conditions. Nearly all water from effective precipitation events between 20 and 30 mm was lost to evaporation between three to four days following the event under similar evaporative demand. Furthermore, the inferred evaporative losses of pre-watering irrigations from precipitation events are likely a liberal estimate in that precipitation events are typically bracketed by atmospheric conditions that are conducive to the condensation of water from the air while irrigations are more likely to occur outside of these conditions. Although the irrigation creates a cooled microclimate at the soil surface during the irrigation, it is short-lived and promptly subjected to higher evaporative demand of the atmosphere. Irrigation system inefficiencies are also not included in the comparisons with effective precipitation. The considerable potential evaporative losses from preseason irrigation provide cause for concern as to whether the practice is a defensible use of limited groundwater resources.

## 5. Disclaimer

The U.S. Department of Agriculture (USDA) prohibits discrimination in all its programs and activities on the basis of race, color, national origin, age, disability, and where applicable, sex, marital status, familial status, parental status, religion, sexual orientation, genetic information, political beliefs, reprisal, or because all or part of an individual's income is derived from any public assistance program. (Not all prohibited bases apply to all programs.) Persons with disabilities who require alternative means for communication of program information (Braille, large print, audiotape, etc.) should contact USDA's TARGET Center at (202) 720–2600 (voice and TDD). To file a complaint of discrimination, write to USDA, Director, Office of Civil Rights.

## References

Allen, R.G., Pruitt, W.O., Raes, D., Smith, M., Periera, L.S., 2005. Estimating evaporation from bares soil and the crop coefficient fotr the initial period using common soils information. J. Irrig. Drain. Eng. 131, 14–23.

ASCE, 2005. The ASCE Standardized Reference Evapotranspiration Equation. Reston, V a: ASCE.

Baumhardt, R.L., Staggenborg, S.A., Gowda, P.A., Colaizzi, P.D., Howell, T.A., 2009. Modeling irrigation management strategies to maximize cotton lint yield and water use efficiency. Agron. J. 101 (3), 460–468.

Baumhardt, R.L., Mauget, S.A., Gowda, P.H., Brauer, D.K., Marek, G.W., 2015. Optimizing cotton irrigation strategies as influenced by El Nino Southern Oscillation. Agron. J., Accepted for publication April 2015.

Dusek, D.A., Howell, T.A., Schneider, A.D., Copeland, K.S., 1987. Bushland weighing lysimeter data aquisition systems for evapotranspiration research. In: ASAE Meeting Paper no. 87-2506, International Winter Meeting of the American Society of Agricultural Engineers, December 15–18, Chicago.

Evett, S.R., Kustas, W.P., Gowda, P.H., Prueger, J.H., Howell, T.A., 2008. Overview of the Bushland evapotranspiration and agricultural remote sensing experiment (BEAREX08): a field experiment evaluating methods quantifying ET at multiple scales. Adv. Water Resour. 50, 4–19, http://dx.doi.org/10.1016/j.advwatres.2012.03.010.

Evett, S.R., Schwartz, R.C., Howell, T.A., Baumhardt, R.L., Copeland, K.S., 2012b. Can weighing lysimeter ET represnt surrounding field ET well enough to test flux station measurements of daily and sub-daily ET? Adv. Water Resour. 50, 79–90.

Evett, S.R., Brauer, D.K., Colaizzi, P.D., O'Shaughnessy, S.A., 2015. Corn and sorghum performance as affected by irrigation application method: SDI versus mid-elevation spray irrigation. In: In Proc. 27th Annual Central Plains Irrigation, Conf., Colby, Kans., February 17–18, pp. 83–95.

Hernandez, J.E., Gowda, P.H., Marek, T.H., Howell, T.A., Wonsook, H., 2013. Groundwater levels in northern Texas High Plains baseline for existing agricultural management practices. Texas Water J. 4 (1), 22–34.

Howell, T.A., Schneider, A.D., Dusek, D.A., Marek, T.H., Steiner, J.L., 1995. Calibration and scale performance of Bushland weighing lysimeters. Trans. ASAE 38 (4), 1019–1024.

Marek, T.H., Schneider, A.D., Howell, T.A., Ebeling, L.L., 1988. Design and construction of large weighing monolithic weighing lysimeters. Trans. ASAE 31 (2), 477–484.

Marek, T.H., Porter, D.O., Howell, T.A., 2005. The Texas High Plains eapotranspiration network—an irrigation scheduling technology transfer tool. Technical report, Texas Water Development Board for contract # 2004-358-008, 16 p.

Marek, G.W., Evett, S.R., Gowda, P.H., Howell, T.A., Copeland, K.S., Baumhardt, R.L., 2014. Post-processing techniques for reducing errors in weighing lysimeter evapotranspiration (ET) datasets. Trans. ASABE 75 (2), 499–515.

Moorhead, J.E., Gowda, P.H., Marek, T.H., Porter, D.O., Howell, T.A., Singh, V.P., Stewart, B.A., 2013. Use of crop-specific drought indices for determing irrigation demand in the Texas High Plains. Appl. Eng. Agric. 29 (6), 905–916.

NRCS, 2015. Official Series Description—PULLMAN Series. <https://soilseries.sc.egov.usda.gov/OSD_Docs/P/PULLMAN.html/> (accessed 01.09.15.).

O'Shaughnessy, S.A., Urrego, Y.F., Evett, S.R., Colaizzi, P.D., Howell, T.A., 2013. Assessing application uniformity of a variable rate irrigation system in a windy location. Appl. Eng. Agric. 29 (4), 497–510.

O'Shaughnessy, S.A., Evett, S.R., Colaizzi, P.D., 2015. Dynamic prescription maps for site-specific variable rate irrigation of cotton. Agric. Water Manag. 159, 123–138.

Pitttman, E.G., Hunt, J., Herring, J.E., Meadows, W.W., Labbat, T.W., Guerra, D.V., 2007. Water for Texas. vol. II. Doc. GP-8-1. Texas Water Development Board, Austin.

Schneider, A.D., Marek, T.H., Ebeling, L.L., Howell, T.A., Steiner, J.L., 1988. Hydraulic pulldown procedure for collecting large soil monliths. Trans. ASAE 31 (2), 1092–1097.

Schwartz, R.C., Baumhardt, R.L., Evett, S.R., 2010. Tillage effects on soil water distrubution and bare soil evaporation throughout a season. Soil Tillage Res. 110, 221–229.

Tolk, J.A., Evett, S.R., Schwartz, R.C., 2015. Field-measured, hourly soil water evaporation stages in relation to reference evapotranspiration rate and soil to air temperature ratio. Vadose Zone J., http://dx.doi.org/10.2136/vzj2014.07. 0079.

Unger, P.W., Pringle, F.B., 1981. Pullman soils: distribution importance, variability, and management. College Station, TX: Texas. Agric. Exp. Station Bull., B-1372.